

## ***Vaccinium bracteatum* Thunb. Exerts Anti-Inflammatory Activity by Inhibiting NF- $\kappa$ B Activation in BV-2 Microglial Cells**

Seung-Hwan Kwon<sup>1</sup>, Shi-Xun Ma<sup>1</sup>, Yong-Hyun Ko<sup>1</sup>, Jee-Yeon Seo<sup>1</sup>, Bo-Ram Lee<sup>1</sup>, Taek Hwan Lee<sup>2</sup>, Sun Yeou Kim<sup>3</sup>, Seok-Yong Lee<sup>1</sup> and Choon-Gon Jang<sup>1,\*</sup>

<sup>1</sup>Department of Pharmacology, School of Pharmacy, Sungkyunkwan University, Suwon 16419,

<sup>2</sup>College of Pharmacy, Yonsei University, Incheon 21983,

<sup>3</sup>College of Pharmacy, Gachon University, Incheon 21936, Republic of Korea

### **Abstract**

This study was designed to evaluate the pharmacological effects of *Vaccinium bracteatum* Thunb. methanol extract (VBME) on microglial activation and to identify the underlying mechanisms of action of these effects. The anti-inflammatory properties of VBME were studied using lipopolysaccharide (LPS)-stimulated BV-2 microglial cells. We measured the production of nitric oxide (NO), inducible NO synthase (iNOS), cyclooxygenase (COX)-2, prostaglandin E<sub>2</sub> (PGE<sub>2</sub>), tumor necrosis factor- $\alpha$  (TNF- $\alpha$ ), interleukin-1 beta (IL-1 $\beta$ ), and interleukin-6 (IL-6) as inflammatory parameters. We also examined the effect of VBME on intracellular reactive oxygen species (ROS) production and the activity of nuclear factor-kappa B p65 (NF- $\kappa$ B p65). VBME significantly inhibited LPS-induced production of NO and PGE<sub>2</sub> and LPS-mediated upregulation of iNOS and COX-2 expression in a dose-dependent manner; importantly, VBME was not cytotoxic. VBME also significantly reduced the generation of the pro-inflammatory cytokines TNF- $\alpha$ , IL-1 $\beta$ , and IL-6. In addition, VBME significantly dampened intracellular ROS production and suppressed NF- $\kappa$ B p65 translocation by blocking I $\kappa$ B- $\alpha$  phosphorylation and degradation in LPS-stimulated BV2 cells. Our findings indicate that VBME inhibits the production of inflammatory mediators in BV-2 microglial cells by suppressing NF- $\kappa$ B signaling. Thus, VBME may be useful in the treatment of neurodegenerative diseases due to its ability to inhibit inflammatory mediator production in activated BV-2 microglial cells.

**Key Words:** *Vaccinium bracteatum* Thunb, Anti-inflammatory activity, Nuclear factor- $\kappa$ B p65, Lipopolysaccharide, BV-2 microglial cells

### **INTRODUCTION**

Microglia, resident macrophages, and immune surveillance cells in the central nervous system (CNS) have all been reported to play a critical role in host defense and tissue repair in the brain (Schwartz, 2003). However, excessive activation of microglia has been proposed to play a pathogenic role in neuro-inflammatory conditions such as Alzheimer's disease (AD), Parkinson's disease (PD), ischemia, and HIV-associated dementia (Amor *et al.*, 2010).

Activation of microglia and the consequent release of pro-inflammatory and/or cytotoxic factors, such as tumor necrosis factor- $\alpha$  (TNF- $\alpha$ ), interleukin-1 beta (IL-1 $\beta$ ), interleukin-6 (IL-6), nitric oxide (NO), prostaglandin E<sub>2</sub> (PGE<sub>2</sub>), and reactive oxygen species (ROS) are believed to contribute to neurodegenerative processes (Block *et al.*, 2007; Lull and Block,

2010). These observations suggest that microglia-derived factors play an important role in neurodegeneration. In addition, the mechanisms that regulate microglial activation may be important therapeutic targets for treating various neurodegenerative diseases such as AD, PD, ischemia, and HIV-associated dementia.

*Vaccinium bracteatum* Thunb. (VB), which belongs to the same genus (*Ericaceae*) as blueberry and is widely grown throughout China and Korea, is used as a traditional Chinese herbal medicine. The physiological activity of VB against fatigue and indigestion and the antioxidant properties of VB have been recorded in the Compendium of Materia Medica. Recently, VB was confirmed to have anti-microbial, anti-oxidant, and anti-fatigue properties, in addition to protecting the retina from light damage (Wang *et al.*, 2010; Wang *et al.*, 2013). The aqueous extract of VB is used to dye rice for patients with

**Open Access** <http://dx.doi.org/10.4062/biomolther.2015.205>

This is an Open Access article distributed under the terms of the Creative Commons Attribution Non-Commercial License (<http://creativecommons.org/licenses/by-nc/4.0/>) which permits unrestricted non-commercial use, distribution, and reproduction in any medium, provided the original work is properly cited.

Received Dec 14, 2015 Revised Mar 3, 2016 Accepted Mar 8, 2016

Published Online Sep 1, 2016

**\*Corresponding Author**

E-mail: jang@skku.edu

Tel: +82-31-290-7780, Fax: +82-31-292-8800

**Table 1.** Primers used in RT-PCR experiments

Target	Forward primer (5' → 3')	Reverse primer (5' → 3')	Size
iNOS	CTGCAGCACTTGGATCAG GAACCTG	GGGAGTAGCCTG TGTGCACCTGGAA	311 bp
COX-2	TTGAAGACCAGGAGTACAGC	GGTACAGTCCATGACATCG	324 bp
TNF- $\alpha$	CGTCAGCCGATTTGCTATCT	CGGACTCCGCAAAGTCTAAG	206 bp
IL-1 $\beta$	GCCCATCCTCTGTGACTCAT	AGGCCACAGGTATTTGTGCG	230 bp
IL-6	CCACTTCACAAGTCGGAGGCTT	CCAGCTTATCTGTTAGGAGA	396 bp
GAPDH	TGATGACATCAAGAAGGTGGTGAAG	TCCTTGAGGCCATGTAGGCCAT	240 bp

diabetes in parts of the eastern coastal region of China so that patients can eat more rice and avoid hunger pains (Wang *et al.*, 2010; Wang *et al.*, 2013). The effects of VB on streptozotocin-induced diabetic mice were also reported recently (Wang *et al.*, 2010; Wang *et al.*, 2013). Although VB extract has been reported to exhibit several bioactivities, the anti-inflammatory effects of VB methanol extract (VBME) on cells in the central nervous system (CNS), specifically microglia, have remained elusive. Indeed, the detailed molecular mechanisms underlying the effects of VBME on neuro-inflammation have not yet been investigated. Therefore, in this study we evaluated the pharmacological effects of VBME on microglial activation. We also identified the underlying mechanism of action by investigating the phosphorylation status of MAPKs, PI3K/Akt, and GSK-3 $\beta$ , in addition to assessing nuclear factor-kappa B p65 (NF- $\kappa$ B p65) activation.

## MATERIALS AND METHODS

### Materials

Ammoniumpyrrolidinedithiocarbamate (PDTC), 2,7'-dichlorofluorescein diacetate (DCFH-DA), dimethyl sulfoxide (DMSO), Hoechst 33258, 3-(4,5-dimethyl thiazol-2-yl)-2,5-diphenyl tetrazolium bromide (MTT), lipopolysaccharide (LPS; *Escherichia coli*, 026:B6), poly-D-lysine, quercetin, and anti- $\beta$ -actin antibodies were purchased from Sigma Chemical Co. (St. Louis, MO, USA). Dulbecco's modified Eagle's medium (DMEM) was obtained from Hyclone (Logan, UT, USA). Fetal bovine serum (FBS), 0.25% trypsin-EDTA, and penicillin/streptomycin were obtained from GIBCO-BRL (Grand Island, NY, USA). Primary antibodies were purchased from Epitomics (Burlingame, CA, USA) and Santa Cruz Biotechnology, Inc. (Santa Cruz, CA, USA). Secondary antibodies were purchased from Jackson ImmunoResearch Laboratories Inc. (West Grove, PA, USA). Alexa Fluor<sup>®</sup> 488-conjugated goat anti-rabbit IgG antibodies and Lipofectamine<sup>®</sup> 2000 transfection reagent were purchased from Invitrogen (Carlsbad, CA, USA). PCR primers were synthesized by Cosmogenetech Co., Ltd. (Seoul, Republic of Korea). All other chemicals were of analytical grade and were purchased from Sigma Chemical Co.

### Preparation of Vaccinium bracteatum Thunb. methanol extract (VBME)

The aboveground parts of VB were collected in Yunnan Province, China, in September 2012. A voucher specimen was deposited in the herbarium of the Korea Research Institute of Bioscience and Biotechnology (KRIBB, Daejeon, Republic of Korea). VB was obtained from the International Biological Ma-

terial Research Center (IBMRC) of KRIBB. Air-dried VB was cut into small pieces and extracted three times with 100 g/L of 95% methanol at 85°C with a cooling system (40°C) for 3 h. The methanol extract was filtered through Whatman No. 2 filter paper (GE Healthcare Life Sciences, Pittsburgh, PA, USA) and the supernatant was concentrated under reduced pressure in a vacuum rotary evaporator (EYELA, N-1000, Tokyo, Japan). Finally, the supernatant was evaporated and spray dried to yield 112 g of VBME. The lyophilized powder was stored at -70°C and dissolved in dimethyl sulfoxide (DMSO) prior to use.

### Cell culture and treatment

BV-2 microglial cells were grown in DMEM supplemented with 10% heat-inactivated FBS (v/v) and 0.1% penicillin/streptomycin (v/v) in a humidified atmosphere of 5% CO<sub>2</sub> and 95% air at 37°C. LPS was prepared immediately before use as a 10  $\mu$ g/ml stock and diluted in PBS to the indicated final concentration. VBME, quercetin, and PDTC were dissolved in DMSO. Stock solutions were added directly to the culture medium. Control cells were treated with DMSO alone. The final concentration of solvent was always <0.1% (v/v). No significant cytotoxicity was observed in any of the experiments (data not shown). In all experiments, cells were treated with the indicated concentrations of VBME, quercetin, and PDTC in serum-free DMEM in the presence or absence of LPS (100 ng/ml).

### Determination of NO production

NO release into the culture supernatants was measured by the Griess reaction. In brief, BV-2 microglial cells (2.5 $\times$ 10<sup>5</sup> cells/well in 24-well plates) were incubated at 37°C with LPS for 24 h with or without VBME or quercetin pretreatment, after which the NO contents of the supernatants were assayed. Specifically, 50  $\mu$ l of culture supernatant was mixed with an equal volume of Griess reagent [0.1% N-(1-naphthyl)-ethylenediamine dihydrochloride and 1% sulfanilamide in 5% phosphoric acid] in a 96-well plate for 10 min at room temperature in the dark. Nitrite concentrations were determined using standard solutions of sodium nitrite prepared in cell culture medium. The absorbance of each well at 540 nm was determined using a microplate reader (SpectraMax M2, Molecular Devices, Sunnyvale, CA, USA).

### Enzyme-linked immunosorbent assay (ELISA)

ELISA kits were used to determine the levels of PGE<sub>2</sub> (Cayman Chemical, Ann Arbor, MI, USA) and TNF- $\alpha$ , IL-1 $\beta$ , and IL-6 (KOMA Biotech Inc., Seoul, Republic of Korea) according to the manufacturer's instructions.

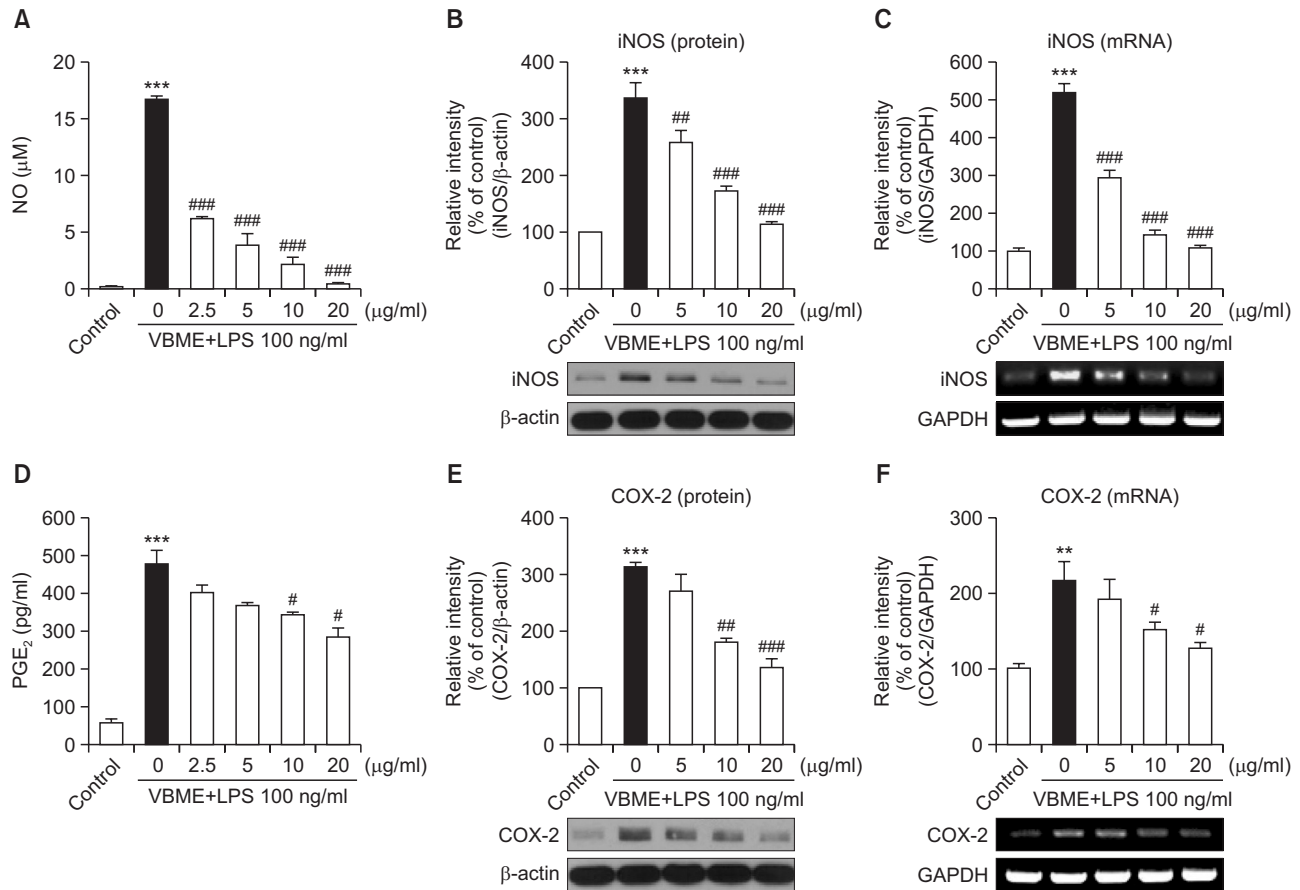


**Fig. 1.** VBME inhibits NO (A) and PGE<sub>2</sub> (D) production in LPS-stimulated BV-2 microglial cells. Cells were pretreated with the indicated concentrations of VBME for 30 min and then exposed to 100 ng/ml LPS for 24 h. The concentration of nitrite in the culture medium was determined using the Griess reagent and the concentration of PGE<sub>2</sub> in the culture medium was measured using a commercial ELISA kit. VBME suppressed LPS-mediated induction of protein and mRNA expression of iNOS (B and C) and COX-2 (E and F) in BV-2 microglial cells. (B and E) Cells were pretreated with the indicated concentrations of VBME for 30 min and then exposed to 100 ng/ml LPS for 24 h. The protein levels of iNOS, COX-2, and  $\beta$ -actin were assessed by Western blot analysis. (C and F) Cells were pretreated with the indicated concentrations of VBME for 30 min and then exposed to 100 ng/ml of LPS for 6 h. The mRNA levels of iNOS, COX-2, and  $\beta$ -actin were determined by RT-PCR. Densitometric results are presented as means  $\pm$  SEMs (n=3) of three independent experiments. \*\* $p$ <0.01 and \*\*\* $p$ <0.001 compared with the control group. # $p$ <0.05, ## $p$ <0.01, and ### $p$ <0.001 compared with the LPS-treated group.

### RNA isolation and reverse transcription-polymerase chain reaction (RT-PCR)

RT-PCR was carried out as previously described Kwon *et al.*, 2015b. Briefly, BV-2 microglial cells ( $1 \times 10^6$  cells/well in 6-well plates) were incubated at 37°C with LPS for 6 h with or without VBME or quercetin pretreatment. Total RNA was isolated using Trizol® reagent (Invitrogen). Reverse transcription reactions were carried out with a Superscript®-III kit (Invitrogen) using 5  $\mu\text{g}$  of total RNA and oligo dT according to the manufacturer's instructions. Band intensities of the amplified DNA fragments were compared after visualization on a UV transilluminator. mRNA band intensities were quantified by densitometric analysis using ImageJ software (NIH Image, public domain, USA). Specific primer sequences are described in Table 1.

### Preparation of nuclear and cytosolic fractions

BV-2 microglial cells were seeded at a density of  $5 \times 10^6$  cells/well in 100 mm<sup>2</sup> cell culture dishes. After pretreatment with VBME for 30 min, the cells were incubated with LPS for 1

h. To measure activation of NF- $\kappa$ B p65 in the nucleus, nuclear and cytosolic fractions were prepared using NE-PER nuclear and cytoplasmic extraction reagents for cultured cells (Pierce, Rockford, IL, USA) according to the manufacturer's instructions.

### Western blot analysis

Western blot analysis was performed as previously described (Kwon *et al.*, 2015a). In brief, BV-2 microglial cells were seeded at a density of  $1 \times 10^6$  cells/well in 6-well plates. After pretreatment with VBME or quercetin for 30 min, the cells were incubated with LPS for 1 h or 24 h. Densitometric analysis was then performed using data obtained from at least three independent experiments. To determine band density, the enhanced chemiluminescence (ECL) approach was used by immersing the probed membrane for 5 min in a 1:1 mixture of ECL reagents A and B (Animal Genetics Inc., Suwon, Republic of Korea). Membranes were then exposed to photographic film for a few minutes. Band intensities were quantified by densitometric analysis using ImageJ software.

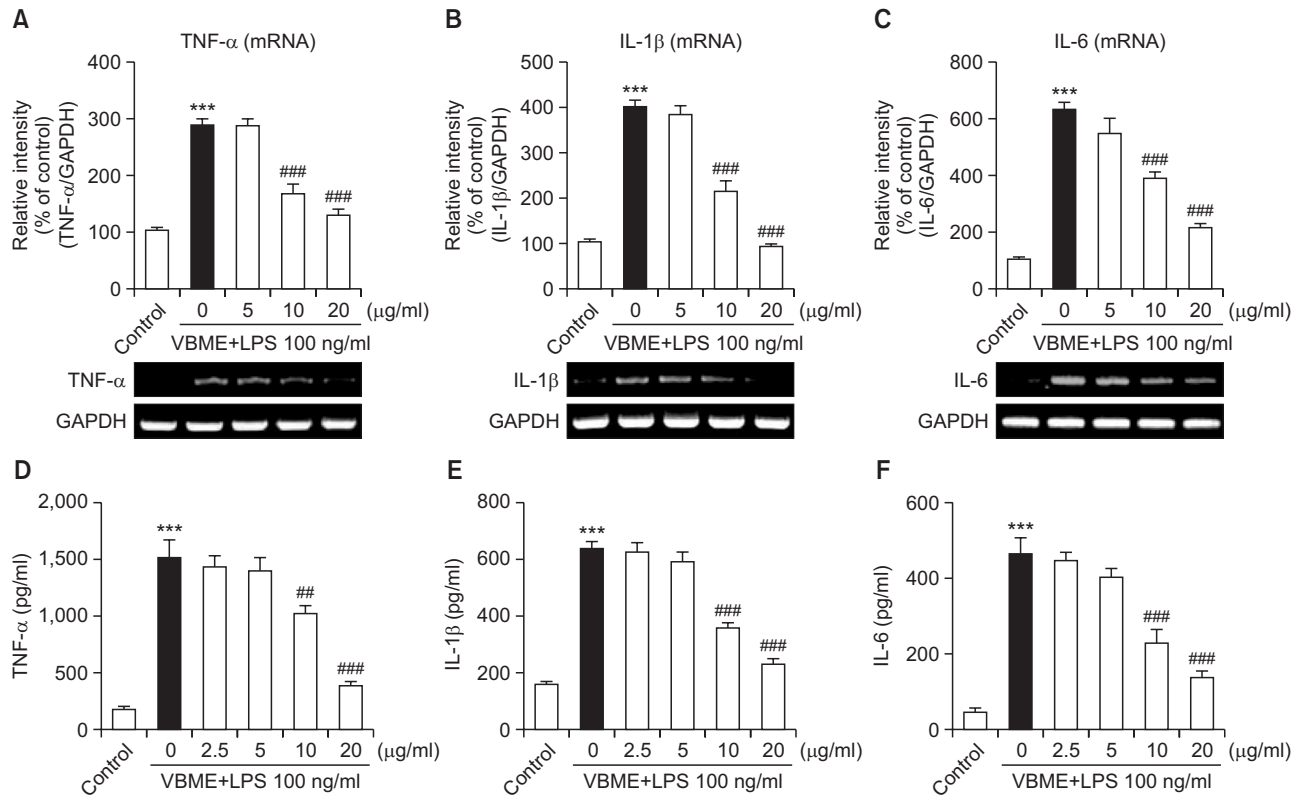


**Fig. 2.** VBME inhibits LPS-mediated induction of TNF- $\alpha$  (A and D), IL-1 $\beta$  (B and E), and IL-6 (C and F) in BV-2 microglial cells. Cells were pretreated with the indicated concentrations of VBME for 30 min and then exposed to 100 ng/ml LPS for 6 h. The mRNA levels of TNF- $\alpha$ , IL-1 $\beta$ , IL-6, and  $\beta$ -actin were evaluated by RT-PCR. Densitometric results are presented as means  $\pm$  SEMs (n=3) of three independent experiments. To quantify cytokine release, cells were pretreated with the indicated concentrations of VBME for 30 min and then exposed to 100 ng/ml LPS for 24 h. The concentrations of TNF- $\alpha$ , IL-1 $\beta$ , and IL-6 in the culture medium were measured using commercial ELISA kits. Data are presented as means  $\pm$  SEMs (n=6). \*\*\* $p$ <0.001 compared with the control group. ## $p$ <0.01 and ### $p$ <0.001 compared with the LPS-treated group.

**Immunocytochemistry**

BV-2 microglial cells ( $2.5 \times 10^5$  cells/well) were cultured on glass coverslips (SPL Lifesciences Co., Pocheon, Korea) for 24 h. After pretreatment with VBME for 30 min, the cells were incubated with LPS for 1 h. Immunocytochemistry was carried out as previously described (Kwon *et al.*, 2015b). Cells were observed under a fluorescence microscope (100 $\times$  magnification). Results shown are representative of three independent experiments.

**Statistics**

All data were analyzed with Prism 5.0 software (GraphPad Software, Inc., San Diego, CA, USA) and are expressed as means  $\pm$  SEMs. Statistical analyses were performed using one-way analysis of variance (ANOVA) followed by the Newman-Keuls test. Statistical significance was set at  $p$ <0.05.

**RESULTS**

**Effect of VBME on the viability of LPS-treated BV-2 microglial cells**

To exclude the possibility that the observed changes were simply due to cell death, we tested cell viability after treatment with various concentrations of VBME (1, 2.5, 5, 10, and 20  $\mu$ g/ml

for 24 h without LPS or for 30 min with LPS). Since VBME had no cytotoxic effects (Fig. S1A, S1B), these concentrations of VBME were used in all subsequent experiments.

**VBME inhibits NO and PGE<sub>2</sub> production in LPS-stimulated BV-2 microglial cells**

We first evaluated the effects of VBME on NO and PGE<sub>2</sub> production in LPS-stimulated BV-2 cells. Treatment with LPS significantly increased NO and PGE<sub>2</sub> production compared with the control treatment (Fig. 1A, 1D,  $p$ <0.001). However, VBME significantly inhibited these LPS-mediated increases in NO and PGE<sub>2</sub> production in a concentration-dependent manner ( $p$ <0.05 and  $p$ <0.001, respectively).

**VBME suppresses LPS-mediated induction of iNOS and COX-2 expression in BV-2 microglial cells**

To investigate whether VBME-mediated inhibition of NO and PGE<sub>2</sub> production involved modulation of iNOS and COX-2 activity, we determined the protein and mRNA levels of these enzymes by Western blotting and RT-PCR, respectively. Treatment with LPS resulted in significantly increased protein levels of iNOS and COX-2 (Fig. 1B, 1E,  $p$ <0.001). However, pretreatment with VBME significantly inhibited LPS-mediated upregulation of iNOS and COX-2 in a concentration-dependent manner ( $p$ <0.01, and  $p$ <0.001, respectively). To examine

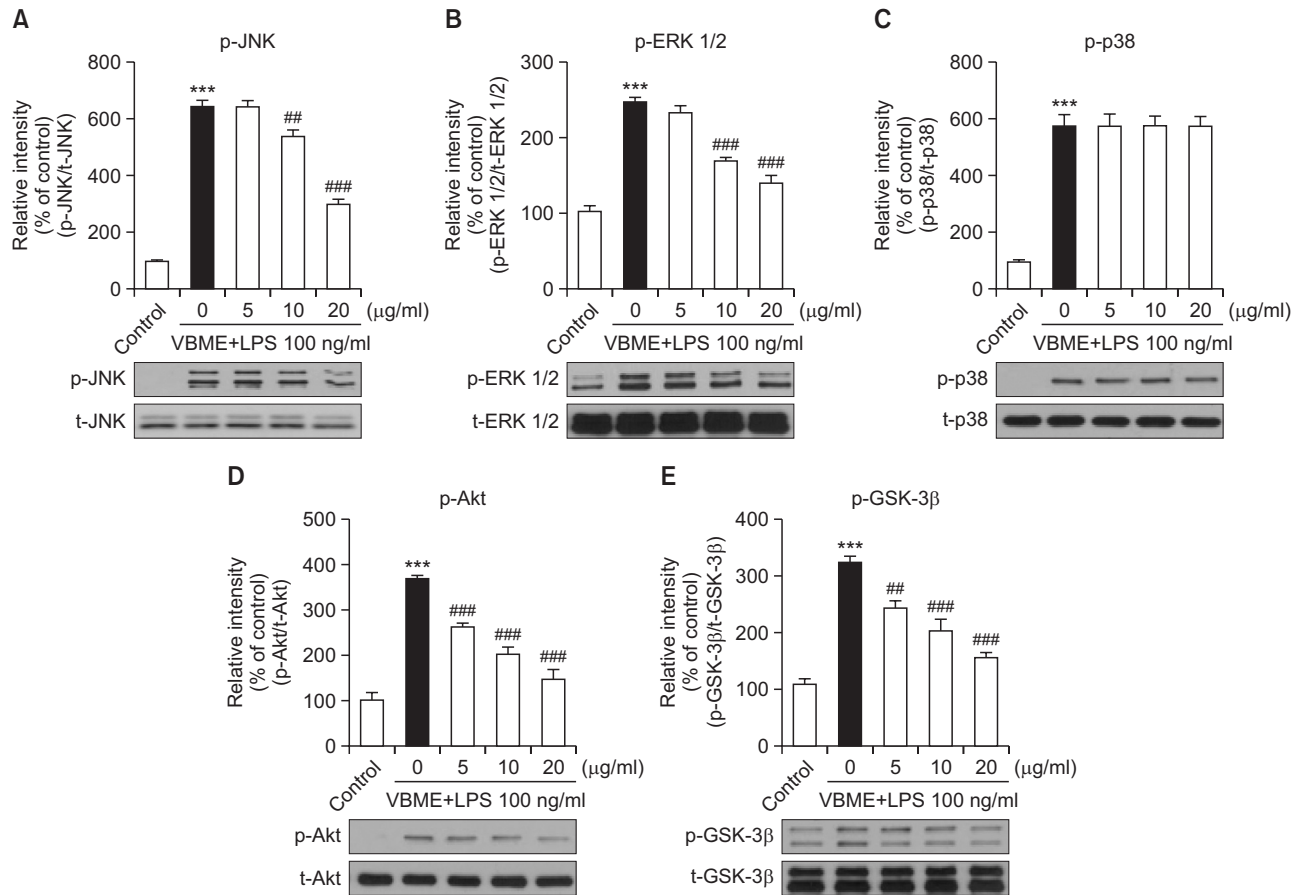


**Fig. 3.** VBME suppresses LPS-induced phosphorylation of JNK (A), ERK 1/2 (B), p38 (C) MAPKs, PI3K/Akt (D), and GSK-3 $\beta$  (E) in BV-2 microglial cells. Cells were pretreated with the indicated concentrations of VBME for 30 min and then exposed to 100 ng/ml LPS for 1 h. The protein levels of JNK, ERK 1/2, p38 MAPKs, PI3K/Akt, and GSK-3 $\beta$  were evaluated by Western blot analysis. Densitometric results are presented as means  $\pm$  SEMs ( $n=3$ ) of three independent experiments. \*\*\* $p<0.001$  compared with the control group. ## $p<0.01$  and ### $p<0.001$  compared with the LPS-treated group.

the effects of VBME on LPS-mediated changes in iNOS and COX-2 expression on the transcriptional level, we performed RT-PCR analysis. As shown in Fig. 1C, 1F, LPS treatment significantly upregulated iNOS and COX-2 mRNA expression ( $p<0.01$  and  $p<0.001$ , respectively). However, pretreatment with VBME significantly inhibited this induction in a concentration-dependent manner ( $p<0.05$  and  $p<0.001$ , respectively).

#### **VBME inhibits LPS-induced production of TNF- $\alpha$ , IL-1 $\beta$ , and IL-6 in BV-2 microglial cells**

We next determined whether VBME inhibits LPS-induced production of TNF- $\alpha$ , IL-1 $\beta$ , and IL-6 using RT-PCR and ELISA. Stimulation of BV-2 cells with LPS induced a significant increase in the mRNA levels of the pro-inflammatory cytokines TNF- $\alpha$ , IL-1 $\beta$ , and IL-6 (Fig. 2A-2C,  $p<0.001$ ); however, pretreatment with VBME inhibited this effect in a dose-dependent manner ( $p<0.001$ ). In a parallel approach, we determined whether VBME inhibited the release of these factors by quantifying cytokine levels in the culture medium by ELISA. Treatment with LPS resulted in significantly increased TNF- $\alpha$ , IL-1 $\beta$ , and IL-6 production compared with the control treatment (Fig. 2D-2F,  $p<0.001$ ). However, pretreatment with VBME inhibited cytokine release in a dose-dependent manner ( $p<0.01$

and  $p<0.001$ , respectively).

#### **VBME inhibits LPS-induced ROS accumulation in BV-2 microglial cells**

We next examined the effect of VBME on ROS, which are known to be early inducers of inflammation. We investigated intracellular ROS formation with DCFH-DA, a fluorescent ROS-sensitive probe. Treatment with LPS resulted in significantly increased intracellular ROS production compared with the control treatment (Fig. S2A,  $p<0.001$ ), whereas pretreatment with VBME significantly inhibited this enhancement of intracellular ROS accumulation in a dose-dependent manner ( $p<0.001$ ). To further investigate the effect of VBME on LPS-induced intracellular ROS accumulation, we visualized DCFH-DA staining on a fluorescence microscope. Microphotographs of DCFH-DA staining revealed excessive intracellular ROS accumulation after LPS stimulation (Fig. S2B). Interestingly, pretreatment with VBME clearly inhibited the signaling events leading to intracellular ROS accumulation.

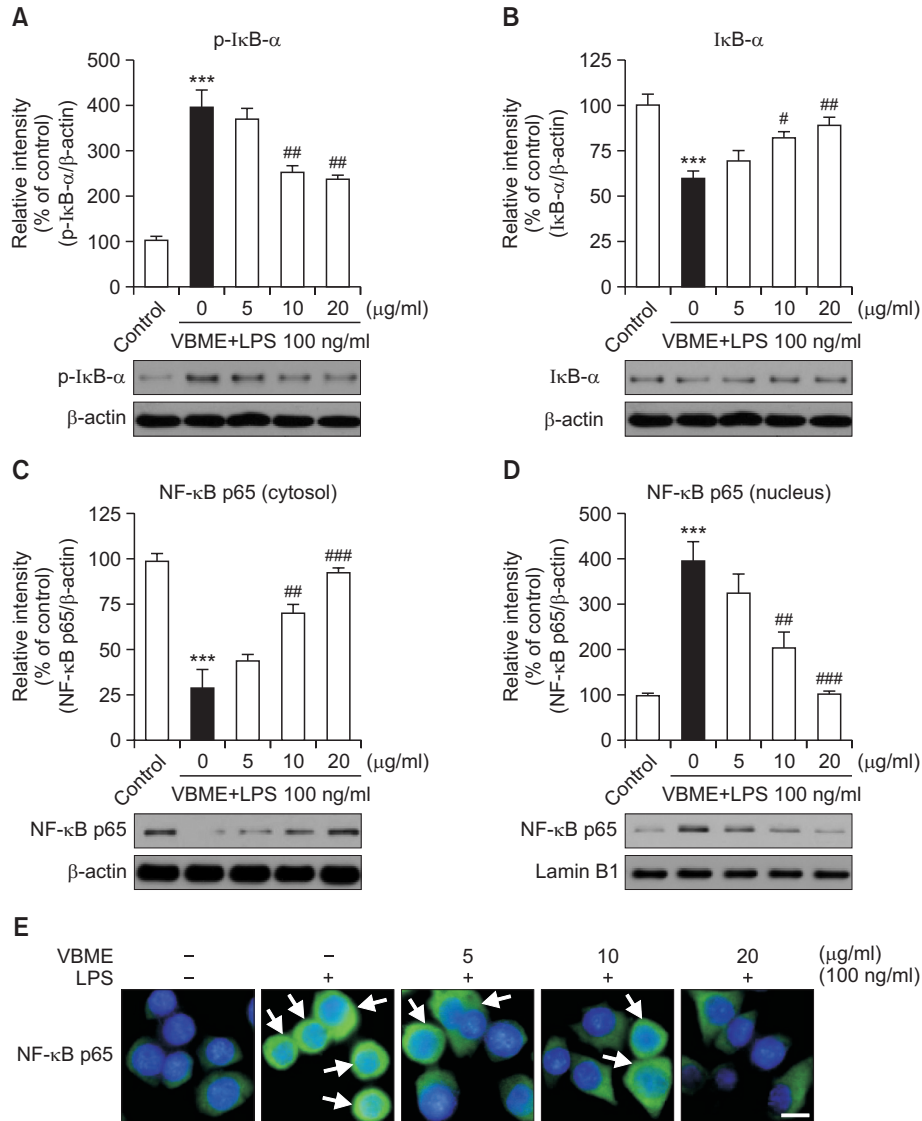


**Fig. 4.** VBME inhibits LPS-induced phosphorylation and degradation of IκB-α (A and B) and NF-κB p65 activation (C and D) in BV-2 microglial cells. Cells were pretreated with the indicated concentrations of VBME for 30 min and then exposed to 100 ng/ml LPS for 1 h. The protein levels of IκB-α, NF-κB p65, β-actin, and lamin B1 were measured by Western blot analysis. Densitometric results are presented as means ± SEMs (n=3) of three independent experiments. Immunofluorescence staining was performed with anti-NF-κB p65 antibodies and Alexa Fluor® 488-conjugated secondary antibodies. Nuclei were counterstained with Hoechst 33258. Representative pictures were taken with a fluorescence microscope (E, 100× magnification). The images shown are representative of three experiments. Scale bar: 200 μm. \*\*\*p<0.001 compared with the control group. #p<0.05, ##p<0.01, and ###p<0.001 compared with the LPS-treated group.

**VBME suppresses LPS-induced phosphorylation of JNK and ERK1/2 MAPKs, PI3K/Akt, and GSK-3β in BV-2 microglial cells**

To evaluate the effect of VBME on the signaling pathway upstream of NF-κB activation, we examined changes in the activation of intracellular signaling proteins in BV-2 cells by Western blot analysis. As shown in Fig. 5, treatment with LPS dramatically and rapidly increased the phosphorylation of JNK, ERK 1/2, p38 MAPKs, PI3K/Akt, and GSK-3β compared with the control treatment (Fig. 3, p<0.001). The LPS-mediated increases in phosphorylation of JNK, ERK 1/2, PI3K/Akt, and GSK-3β were significantly inhibited by VBME in a dose-dependent manner (p<0.01 and p<0.001), whereas the phos-

phorylation of p38 was not significantly affected.

**VBME inhibits LPS-induced phosphorylation and degradation of IκB-α and activation of NF-κB p65 in BV-2 microglial cells**

Since NF-κB is one of the most important transcription factors that regulate gene expression of pro-inflammatory mediators, we tested the effects of VBME on LPS-mediated activation of NF-κB p65 by Western blot and immunocytochemistry assays. Treatment with LPS resulted in significantly increased phosphorylation of IκB-α compared with the control treatment (Fig. 4A, p<0.001), whereas IκB-α exhibited significantly increased degradation upon control stimulation compared with

LPS stimulation (Fig. 4B,  $p < 0.001$ ). This increase in phosphorylation of I $\kappa$ B- $\alpha$  was significantly inhibited by VBME ( $p < 0.01$ ). Pretreatment with VBME also significantly inhibited I $\kappa$ B- $\alpha$  degradation compared with LPS treatment ( $p < 0.05$  and  $p < 0.01$ ). Treatment with LPS resulted in significant translocation of NF- $\kappa$ B p65 from the cytoplasm to the nucleus (Fig. 4C, 4D,  $p < 0.001$ ). However, LPS-mediated translocation of NF- $\kappa$ B was significantly inhibited by VBME ( $p < 0.01$  and  $p < 0.001$ ).

Considering the inhibitory effects of VBME on LPS-mediated translocation of NF- $\kappa$ B p65, we measured the activation of NF- $\kappa$ B p65 transcriptional activity using a luciferase reporter assay in BV-2 microglial cells. As shown in Fig. S3A, treatment with LPS significantly increased the activity of NF- $\kappa$ B p65 compared with the control treatment ( $p < 0.001$ ). However, activation of NF- $\kappa$ B p65 was significantly inhibited by VBME ( $p < 0.001$ ). Immunocytochemistry analysis revealed that NF- $\kappa$ B p65 was normally sequestered in the cytoplasm, whereas robust nuclear accumulation of NF- $\kappa$ B p65 was observed in BV-2 microglial cells following stimulation with LPS. Moreover, LPS-mediated nuclear translocation of NF- $\kappa$ B p65 was inhibited in a concentration-dependent manner by pretreatment with VBME (Fig. 4E). In accordance with the EMSA results, treatment with LPS significantly increased the DNA-binding activity of NF- $\kappa$ B (Fig. S3B). In contrast, pretreatment with VBME or PDTC, a specific NF- $\kappa$ B inhibitor, significantly suppressed this LPS-mediated increase in NF- $\kappa$ B DNA-binding activity.

#### HPLC analysis of VBME and effects of the active constituent of VBME on pro-inflammatory responses in LPS-stimulated BV-2 microglial cells

HPLC analysis of VBME showed several peaks, indicating a diverse mixture of compounds. Although the areas of the peaks obtained were below the limit of quantification, we compared them with the reference standard quercetin (Fig. S4A). By comparison of retention times and UV spectra, we identified quercetin as one of the major constituents of VBME (Fig. S4B). To further confirm the anti-inflammatory effects of quercetin on NO production, PGE<sub>2</sub> production, iNOS expression, and COX-2 expression, BV-2 microglial cells were pretreated with the indicated concentrations of quercetin and then stimulated with LPS. Treatment with LPS resulted in significantly increased NO and PGE<sub>2</sub> production compared with the control treatment (Fig. S4C, S4F,  $p < 0.001$ ). However, these increases in NO and PGE<sub>2</sub> production were significantly inhibited by quercetin in a concentration-dependent manner ( $p < 0.01$  and  $p < 0.001$ , respectively). In addition, treatment with LPS resulted in significantly elevated protein levels of iNOS and COX-2 (Fig. S4D, S4G,  $p < 0.001$ ). However, pretreatment with quercetin significantly inhibited these effects in a concentration-dependent manner ( $p < 0.05$ ,  $p < 0.01$ , and  $p < 0.001$ , respectively). To further examine the effects of quercetin on LPS-mediated upregulation of iNOS and COX-2 expression, we performed RT-PCR analysis. As shown in Fig. S4E and S4H, treatment with LPS significantly induced the expression of iNOS and COX-2 mRNA ( $p < 0.001$ ). However, pretreatment with quercetin significantly inhibited this induction in a concentration-dependent manner ( $p < 0.05$  and  $p < 0.001$ , respectively). Quercetin was not cytotoxic at the concentrations used here (data not shown); therefore, the same concentrations of VBME were used in these experiments.

## DISCUSSION

NO and PGE<sub>2</sub> are key inflammatory and neurotoxic mediators in neuro-inflammation that are responsible for the detrimental effects of injury and/or disease state on the CNS. These mediators act in the context of many pathological states, including AD, PD, and ischemia (Kim *et al.*, 2013). Many studies have revealed that the abnormally high levels of NO and PGE<sub>2</sub> found in various types of brain injuries and neurodegenerative diseases are caused by dramatic upregulation of iNOS and COX-2 enzymes (Teismann *et al.*, 2003; Lull and Block, 2010; Cunningham, 2013). In the present study, VBME significantly inhibited the production of both NO and PGE<sub>2</sub> by downregulating iNOS and COX-2 expression on both the protein and mRNA levels. Together, these results suggest that VBME is a promising target for inhibiting early steps in inflammatory pathways.

TNF- $\alpha$ , IL-1 $\beta$ , and IL-6 are the major pro-inflammatory cytokines produced by activated microglia during CNS inflammation. Overproduction of these cytokines has been linked to many neurodegenerative diseases, including AD, PD, and multiple sclerosis (Lue *et al.*, 2001; Tansey *et al.*, 2007; Wilms *et al.*, 2007). The overproduction of these pro-inflammatory cytokines by activated microglial cells also has a detrimental effect on neuronal cells. Thus, inhibition of cytokine production and/or function serves as a key mechanism in the control of CNS inflammation. Accordingly, here we investigated whether VBME inhibits LPS-induced production of pro-inflammatory cytokines in BV-2 microglial cells. Our data show that VBME significantly inhibits LPS-induced mRNA upregulation and LPS-induced secretion of TNF- $\alpha$ , IL-1 $\beta$ , and IL-6. Thus, our data indicate that VBME inhibits the production of pro-inflammatory cytokines on the transcriptional level.

ROS accumulation is strongly associated with microglial neuro-inflammation in neurodegenerative diseases. Accordingly, natural anti-oxidant defense mechanisms in microglial cells normally maintain low levels of intracellular ROS. However, during chronic neuro-inflammation ROS amplify neuro-inflammatory signals in microglia through phosphorylation of MAPKs (e.g., JNK, ERK 1/2, and p38), PI3K/Akt, and GSK-3 $\beta$ , as well as through activation of NF- $\kappa$ B and overexpression of pro-inflammatory molecules (Bauer and Bauer, 2002; Park *et al.*, 2012). To evaluate whether the inhibitory effects of VBME on intracellular ROS accumulation are related to upstream MAPKs/PI3K/Akt/GSK-3 $\beta$  phosphorylation and/or NF- $\kappa$ B activation, we examined intracellular ROS production in BV-2 microglial cells. Our results indicated that VBME significantly inhibited LPS-induced intracellular ROS production in BV-2 microglial cells, suggesting a possible mechanism for the inhibitory effects of VBME on MAPKs/PI3K/Akt/GSK-3 $\beta$  phosphorylation and NF- $\kappa$ B activation. Furthermore, VBME-mediated inhibition of ROS generation could potentially inhibit signaling pathway-dependent production of pro-inflammatory mediators and/or cytokines, thereby suppressing neuro-inflammation.

Various intracellular signaling pathways such as the MAPKs, PI3K/Akt, and GSK-3 $\beta$  pathways have previously been reported to be involved in the induction of inflammatory mediators (Kim *et al.*, 2004; Jayasooriya *et al.*, 2014; Ko *et al.*, 2014; Zhao *et al.*, 2014). Phosphorylation of these molecules ultimately upregulates the expression of pro-inflammatory mediators, especially cytokines (Liu *et al.*, 2010). However, un-

regulated phosphorylation of MAPKs, PI3K/Akt, and GSK-3 $\beta$  signaling proteins results in excessive production of inflammatory molecules, which has adverse consequences. Therefore, we performed further experiments to test our hypothesis that VBME tightly regulates the expression of MAPKs to induce anti-inflammatory effects in LPS-stimulated microglial cells. Our results indicated that VBME is a potent inhibitor of phosphorylation of JNK, ERK 1/2 MAPKs, PI3K/Akt, and GSK-3 $\beta$ . However, VBME did not significantly affect LPS-mediated phosphorylation of p38 MAPK. Together, these findings suggest that VBME is capable of disrupting key signal transduction pathways that are activated by LPS in BV-2 microglial cells, thereby preventing the production of neuro-inflammatory molecules.

NF- $\kappa$ B is an essential and ubiquitous transcription factor that drives the expression of many inflammation-related genes, including iNOS, COX-2, TNF- $\alpha$ , IL-1 $\beta$ , and IL-6 (Wang *et al.*, 2002; Ko *et al.*, 2010). NF- $\kappa$ B is retained in the cytoplasm of unstimulated cells by binding to its endogenous inhibitor, I $\kappa$ B- $\alpha$ . NF- $\kappa$ B is activated via phosphorylation and degradation of I $\kappa$ B- $\alpha$ , resulting in the release and nuclear translocation of active NF- $\kappa$ B (Prasad *et al.*, 2015). In the present study, LPS stimulation resulted in nuclear translocation of NF- $\kappa$ B p65 in BV-2 microglial cells. However, pretreatment with VBME suppressed I $\kappa$ B- $\alpha$  degradation and NF- $\kappa$ B activation. Therefore, VBME-mediated inhibition of NF- $\kappa$ B signaling pathways in BV-2 microglial cells might lead to down-regulation of pro-inflammatory mediators, thereby resulting in an anti-inflammatory effect.

The anti-inflammatory effects of VBME are most likely mediated by specific compounds present in this extract. The major active constituents that have been identified in VB leaves are phenolic compounds, including quercetin, chrysin, apigenin, kaempferol, and luteolin (Wang *et al.*, 2013). In our preliminary studies, we found that VBME ameliorates scopolamine-induced and amyloid beta-induced learning and memory impairment, as measured by Y-maze and passive avoidance behavioral performance tests (data not shown). Although we did not assay brain tissue for the presence of VBME, other studies have demonstrated that phenolic compounds present in VBME, including quercetin, chrysin, apigenin, kaempferol, and luteolin, are generally able to penetrate the blood-brain barrier and can be detected in brain tissue (Dajas *et al.*, 2003; Lee *et al.*, 2012). Thus, it is reasonable to conclude that circulating VBME has access to the microglial cell compartment. We note that HPLC analysis of the VB extract used in this study identified quercetin as a peak, based on comparison with a VBME standard (Fig. 6A, 6B).

Quercetin, a flavonoid polyphenolic compound found in many natural herbs, has been shown to exert neuroprotective effects in both *in vivo* and *in vitro* neurodegenerative models; these effects are probably due to its anti-oxidant and anti-inflammatory effects (Zbarsky *et al.*, 2005; Ahmad *et al.*, 2011; Richetti *et al.*, 2011; Xi *et al.*, 2012; Kim *et al.*, 2014). Therefore, quercetin might act either independently or synergistically by regulating multiple signaling pathways to block neuro-inflammation. However, the precise concentrations of these compounds in VBME extract that are required to reach the brain to produce beneficial effects remain unknown and will require further research.

In summary, the results presented here demonstrate that VBME exerts potent anti-inflammatory effects in BV-2 micro-

glial cells. In LPS-stimulated BV-2 microglial cells, VBME significantly inhibited the production of the inflammatory mediators NO and PGE<sub>2</sub> and also suppressed the expression and release of inflammatory molecules such as iNOS, COX-2, TNF- $\alpha$ , IL-1 $\beta$ , and IL-6. These inhibitory effects were associated with VBME-mediated suppression of phosphorylation of MAPKs, PI3K/Akt, and GSK-3 $\beta$ , in addition to VBME-mediated suppression of NF- $\kappa$ B p65 activation. Our results suggest that VBME is a potential therapeutic agent for the treatment of inflammation in neurodegenerative diseases such as AD, PD, and stroke.

To further test the therapeutic potential of VBME for treating neurodegenerative diseases such as AD and PD, the neuroprotective effects of VBME should be further investigated in *in vivo* models. Although we did not evaluate whether VBME inhibits inflammation-related neuronal damage *in vivo*, we demonstrated that VBME exerts anti-inflammatory activity in BV-2 microglial cells. Therefore, further studies are needed to elucidate the precise activities of VBME and its major compounds *in vivo*. We are currently working to isolate other active components of VBME using an activity-guided fractionation approach. Moreover, to confirm that the neuroprotective effects of VBME involve multiple signaling pathways, we are studying the effects of VBME and several of its fractions in mouse models of AD, including models in which neurotoxins such as A $\beta$  are regionally injected into the brain.

## CONFLICT OF INTEREST

The authors declare that there are no conflicts of interest.

## ACKNOWLEDGMENTS

This research was supported by the Basic Science Research Program through the National Research Foundation of Korea (NRF), funded by the Ministry of Science, ICT and Future Planning, Republic of Korea government (NRF-2011-00503 and MRC-2012R1A5A2A28671860).

## REFERENCES

- Ahmad, A., Khan, M. M., Hoda, M. N., Raza, S. S., Khan, M. B., Javed, H., Ishrat, T., Ashafaq, M., Ahmad, M. E., Safhi, M. M. and Islam, F. (2011) Quercetin protects against oxidative stress associated damages in a rat model of transient focal cerebral ischemia and reperfusion. *Neurochem. Res.* **36**, 1360-1371.
- Amor, S., Puentes, F., Baker, D. and van der Valk, P. (2010) Inflammation in neurodegenerative diseases. *Immunology* **129**, 154-169.
- Bauer, M. and Bauer, I. (2002) Heme oxygenase-1: redox regulation and role in the hepatic response to oxidative stress. *Antioxid. Redox. Signal.* **4**, 749-758.
- Block, M. L., Zecca, L. and Hong, J. S. (2007) Microglia-mediated neurotoxicity: uncovering the molecular mechanisms. *Nat. Rev. Neurosci.* **8**, 57-69.
- Cunningham, C. (2013) Microglia and neurodegeneration: the role of systemic inflammation. *Glia* **61**, 71-90.
- Dajas, F., Rivera, F., Blasina, F., Arredondo, F., Echeverry, C., Lafon, L., Morquieo, A. and Heinzen, H. (2003) Cell culture protection and *in vivo* neuroprotective capacity of flavonoids. *Neurotox. Res.* **5**, 425-432.
- Jayasooriya, R. G., Lee, K. T., Lee, H. J., Choi, Y. H., Jeong, J. W. and Kim, G. Y. (2014) Anti-inflammatory effects of  $\beta$ -hydroxyisovaleryl-



- shikonin in BV2 microglia are mediated through suppression of the PI3K/Akt/NF- $\kappa$ B pathway and activation of the Nrf2/HO-1 pathway. *Food Chem. Toxicol.* **65**, 82-89.
- Kim, B. W., Koppula, S., Park, S. Y., Hwang, J. W., Park, P. J., Lim, J. H. and Choi, D. K. (2014) Attenuation of inflammatory-mediated neurotoxicity by *Saururus chinensis* extract in LPS-induced BV-2 microglia cells via regulation of NF- $\kappa$ B signaling and anti-oxidant properties. *BMC Complement. Altern. Med.* **14**, 502.
- Kim, S., Kim, J. I., Choi, J. W., Kim, M., Yoon, N. Y., Choi, C. G., Choi, J. S. and Kim, H. R. (2013) Anti-inflammatory effect of hexane fraction from *Myagropsis myagroides* ethanolic extract in lipopolysaccharide-stimulated BV-2 microglial cells. *J. Pharm. Pharmacol.* **65**, 895-906.
- Kim, S. H., Smith, C. J. and Van Eldik, L. J. (2004) Importance of MAPK pathways for microglial pro-inflammatory cytokine IL-1 beta production. *Neurobiol. Aging* **25**, 431-439.
- Ko, C. Y., Wang, W. L., Wang, S. M., Chu, Y. Y., Chang, W. C. and Wang, J. M. (2014) Glycogen synthase kinase-3 $\beta$ -mediated CCAAT/enhancer-binding protein delta phosphorylation in astrocytes promotes migration and activation of microglia/macrophages. *Neurobiol. Aging* **35**, 24-34.
- Ko, H. M., Koppula, S., Kim, B. W., Kim, I. S., Hwang, B. Y., Suk, K., Park, E. J. and Choi, D. K. (2010) Inflexin attenuates proinflammatory responses and nuclear factor-kappaB activation in LPS-treated microglia. *Eur. J. Pharmacol.* **633**, 98-106.
- Kwon, S. H., Hong, S. I., Ma, S. X., Lee, S. Y. and Jang, C. G. (2015a) 3',4',7-Trihydroxyflavone prevents apoptotic cell death in neuronal cells from hydrogen peroxide-induced oxidative stress. *Food Chem. Toxicol.* **80**, 41-51.
- Kwon, S. H., Ma, S. X., Hong, S. I., Lee, S. Y. and Jang, C. G. (2015b) *Lonicera japonica* THUNB. Extract Inhibits Lipopolysaccharide-Stimulated Inflammatory Responses by Suppressing NF- $\kappa$ B Signaling in BV-2 Microglial Cells. *J. Med. Food* **18**, 762-775.
- Lee, K., Lee, J. S., Jang, H. J., Kim, S. M., Chang, M. S., Park, S. H., Kim, K. S., Bae, J., Park, J. W., Lee, B., Choi, H. Y., Jeong, C. H. and Bu, Y. (2012) Chlorogenic acid ameliorates brain damage and edema by inhibiting matrix metalloproteinase-2 and 9 in a rat model of focal cerebral ischemia. *Eur. J. Pharmacol.* **689**, 89-95.
- Liu, H. T., Du, Y. G., He, J. L., Chen, W. J., Li, W. M., Yang, Z., Wang, Y. X. and Yu, C. (2010) Tetramethylpyrazine inhibits production of nitric oxide and inducible nitric oxide synthase in lipopolysaccharide-induced N9 microglial cells through blockade of MAPK and PI3K/Akt signaling pathways, and suppression of intracellular reactive oxygen species. *J. Ethnopharmacol.* **129**, 335-343.
- Lue, L. F., Walker, D. G. and Rogers, J. (2001) Modeling microglial activation in Alzheimer's disease with human postmortem microglial cultures. *Neurobiol. Aging* **22**, 945-956.
- Lull, M. E. and Block, M. L. (2010) Microglial activation and chronic neurodegeneration. *Neurotherapeutics* **7**, 354-365.
- Park, S. Y., Jin, M. L., Kim, Y. H., Kim, Y. and Lee, S. J. (2012) Anti-inflammatory effects of aromatic-turmerone through blocking of NF- $\kappa$ B, JNK, and p38 MAPK signaling pathways in amyloid  $\beta$ -stimulated microglia. *Int. Immunopharmacol.* **14**, 13-20.
- Prasad, R. G., Choi, Y. H. and Kim, G. Y. (2015) Shikonin Isolated from *Lithospermum erythrorhizon* Downregulates Proinflammatory Mediators in Lipopolysaccharide-Stimulated BV2 Microglial Cells by Suppressing Crosstalk between Reactive Oxygen Species and NF- $\kappa$ B. *Biomol. Ther. (Seoul)* **23**, 110-118.
- Richetti, S. K., Blank, M., Capiotti, K. M., Piato, A. L., Bogo, M. R., Vianna, M. R. and Bonan, C. D. (2011) Quercetin and rutin prevent scopolamine-induced memory impairment in zebrafish. *Behav. Brain Res.* **217**, 10-15.
- Schwartz, M. (2003) Macrophages and microglia in central nervous system injury: are they helpful or harmful? *J. Cereb. Blood Flow Metab.* **23**, 385-394.
- Tansey, M. G., McCoy, M. K. and Frank-Cannon, T. C. (2007) Neuroinflammatory mechanisms in Parkinson's disease: potential environmental triggers, pathways, and targets for early therapeutic intervention. *Exp. Neurol.* **208**, 1-25.
- Teismann, P., Tieu, K., Cohen, O., Choi, D. K., Wu, D. C., Marks, D., Vila, M., Jackson-Lewis, V. and Przedborski, S. (2003) Pathogenic role of glial cells in Parkinson's disease. *Mov. Disord.* **18**, 121-129.
- Wang, L., Zhang, X. T., Zhang, H. Y., Yao, H. Y. and Zhang, H. (2010) Effect of *Vaccinium bracteatum* Thunb. leaves extract on blood glucose and plasma lipid levels in streptozotocin-induced diabetic mice. *J. Ethnopharmacol.* **130**, 465-469.
- Wang, L., Zhang, Y., Xu, M., Wang, Y., Cheng, S., Liebrecht, A., Qian, H., Zhang, H. and Qi, X. (2013) Anti-diabetic activity of *Vaccinium bracteatum* Thunb. leaves' polysaccharide in STZ-induced diabetic mice. *Int. J. Biol. Macromol.* **61**, 317-321.
- Wang, M. J., Lin, W. W., Chen, H. L., Chang, Y. H., Ou, H. C., Kuo, J. S., Hong, J. S. and Jeng, K. C. (2002) Silymarin protects dopaminergic neurons against lipopolysaccharide-induced neurotoxicity by inhibiting microglia activation. *Eur. J. Neurosci.* **16**, 2103-2112.
- Wilms, H., Zecca, L., Rosenstiel, P., Sievers, J., Deuschl, G. and Lucius, R. (2007) Inflammation in Parkinson's diseases and other neurodegenerative diseases: cause and therapeutic implications. *Curr. Pharm. Des.* **13**, 1925-1928.
- Xi, J., Zhang, B., Luo, F., Liu, J. and Yang, T. (2012) Quercetin protects neuroblastoma SH-SY5Y cells against oxidative stress by inhibiting expression of Kruppel-like factor 4. *Neurosci. Lett.* **527**, 115-120.
- Zbarsky, V., Datla, K. P., Parkar, S., Rai, D. K., Aruoma, O. I. and Dexter, D. T. (2005) Neuroprotective properties of the natural phenolic antioxidants curcumin and naringenin but not quercetin and fisetin in a 6-OHDA model of Parkinson's disease. *Free Radic. Res.* **39**, 1119-1125.
- Zhao, M., Zhou, A., Xu, L. and Zhang, X. (2014) The role of TLR4-mediated PTEN/PI3K/AKT/NF- $\kappa$ B signaling pathway in neuroinflammation in hippocampal neurons. *Neuroscience* **269**, 93-101.